

# 1 Introduction to the French GEOTRACES North Atlantic Transect

## 2 (GA01): GEOVIDE cruise

3

4 Sarthou Géraldine <sup>1</sup>, Lherminer Pascale <sup>2</sup>, Achterberg Eric P. <sup>3</sup>, Alonso-Pérez Fernando <sup>4</sup>,  
5 Bucciarelli Eva <sup>1</sup>, Boutorh Julia <sup>1</sup>, Bouvier Vincent <sup>5</sup>, Boyle Edward A. <sup>6</sup>, Branellec Pierre <sup>2</sup>,  
6 Carracedo Lidia I. <sup>4</sup>, Casacuberta Nuria <sup>7</sup>, Castrillejo Maxi <sup>7,8</sup>, Cheize Marie <sup>1,9</sup>, Contreira Pereira  
7 Leonardo <sup>10</sup>, Cossa Daniel <sup>11</sup>, Daniault Nathalie <sup>2</sup>, De Saint-Léger Emmanuel <sup>12</sup>, Dehairs Frank <sup>13</sup>,  
8 Deng Feifei <sup>14</sup>, Desprez de Gésincourt Floriane <sup>1,2</sup>, Devesa Jérémy <sup>1</sup>, Foliot Lorna <sup>15</sup>, Fonseca-  
9 Batista Debany <sup>13,16</sup>, Gallinari Morgane <sup>1</sup>, García-Ibáñez Maribel I. <sup>4,17</sup>, Gourain Arthur <sup>1,18</sup>,  
10 Grossteffan Emilie <sup>19</sup>, Hamon Michel <sup>2</sup>, Heimbürger Lars Eric <sup>20</sup>, Henderson Gideon M. <sup>14</sup>,  
11 Jeandel Catherine <sup>5</sup>, Kermabon Catherine <sup>2</sup>, Lacan François <sup>5</sup>, Le Bot Philippe <sup>2</sup>, Le Goff Manon  
12 <sup>1</sup>, Le Roy Emilie <sup>5</sup>, Lefèbvre Alison <sup>2</sup>, Leizour Stéphane <sup>2</sup>, Lemaitre Nolwenn <sup>1,13,21</sup>, Masqué Pere  
13 <sup>8,22,23</sup>, Ménage Olivier <sup>2</sup>, Menzel Barraqueta Jan-Lukas <sup>3,24</sup>, Mercier Herlé <sup>2</sup>, Perault Fabien <sup>12</sup>,  
14 Pérez Fiz F. <sup>4</sup>, Planquette Hélène F. <sup>1</sup>, Planchon Frédéric <sup>1</sup>, Roukaerts Arnout <sup>13</sup>, Sanial Virginie  
15 <sup>5,25</sup>, Sauzède Raphaëlle <sup>26</sup>, Shelley Rachel U. <sup>1,27</sup>, Stewart Gillian <sup>28,29</sup>, Sutton Jill N. <sup>1</sup>, Tang Yi <sup>28,29</sup>,  
16 Tisnérat-Laborde Nadine <sup>15</sup>, Tonnard Manon <sup>1,30,31</sup>, Tréguer Paul <sup>1</sup>, van Beek Pieter <sup>5</sup>, Zurbrick  
17 Cheryl M. <sup>6</sup>, Zunino Patricia <sup>2</sup>

18

19 1 CNRS, Univ. Brest, IRD, Ifremer, LEMAR (Laboratoire des Sciences de l'environnement  
20 marin), Technopôle Brest-Iroise, 29280 Plouzané, France

21 2 Ifremer, Univ. Brest, CNRS, IRD, Laboratoire d'Océanographie Physique et Spatiale (LOPS),  
22 IUEM, Plouzané, France

23 3 GEOMAR Helmholtz Centre for Ocean Research Kiel, 24124 Kiel, Germany

24 4 Instituto de Investigaciones Marinas, IIM-CSIC, Eduardo Cabello 6, 36208 Vigo, Spain

25 5 LEGOS (Laboratoire d'Etudes en Géophysique et Océanographie Spatiales), Université de  
26 Toulouse, CNRS, CNES, IRD, UPS, 14 Avenue Edouard Belin, 31400 Toulouse, France

27 6 Earth, Atmospheric and Planetary Sciences, Massachusetts Institute of Technology,  
28 Cambridge, MA 02139, USA

29 7 Laboratory of Ion Beam Physics, Department of Earth Sciences, Institute of Geochemistry  
30 and Petrology, ETH-Zurich, Otto Stern Weg 5, Zurich, 8093, Switzerland

31 8 Institut de Ciència i Tecnologia Ambientals & Departament de Física, Universitat Autònoma  
32 de Barcelona, Bellaterra, 08193, Spain

33 9 *Currently at* Laboratoire des cycles géochimiques, Géosciences Marines, Centre Ifremer  
34 Bretagne

35 10 Laboratório de Hidroquímica-IO/FURG, Rio Grande, Brazil

36 11 ISTERRE, Université Grenoble Alpes, CS 40700, 38058 GRENOBLE Cedex 9, France

37 12 CNRS, INSU, Division Technique Bâtiment IPEV - Centre Ifremer, Technopôle Brest-Iroise,  
38 CS 50074, 29280 Plouzané, France

39 13 Analytical, Environmental and Geo-Chemistry, Vrije Universiteit Brussel, Pleinlaan 2, 1050,  
40 Brussels, Belgium

41 14 Department of Earth Sciences, University of Oxford, South Parks Road, Oxford OX13AN, UK

42 15 LSCE/IPSL--CEA-CNRS-UVSQ--Université Paris Saclay, F-91198 Cedex, France

43 16 Department of Biology, Dalhousie University, Halifax, Nova Scotia B3H 4R2, Canada

44 17 Uni Research Climate, Bjerknes Centre for Climate Research, Bergen 5008, Norway  
45 18 Ocean Sciences Department, School of Environmental Sciences, University of Liverpool,  
46 Liverpool, 11 L69 3GP, UK  
47 19 IUEM, UMS 3113, CNRS, Univ. Brest, IRD, Ifremer, Technopôle Brest Iroise, rue Dumont  
48 d'Urville, 29280 PLOUZANE  
49 20 Aix Marseille Université, CNRS/INSU, Université de Toulon, IRD, Mediterranean Institute of  
50 Oceanography UM 110, Marseille, France  
51 21 *Currently at* Department of Earth Sciences, Institute of Geochemistry and Petrology, ETH  
52 Zurich, Zürich, Switzerland  
53 22 Departament de Física, Universitat Autònoma de Barcelona, Bellaterra, 08193, Spain  
54 23 School of Science, Centre for Marine Ecosystems Research, Edith Cowan University,  
55 Joondalup, WA 6027, Australia  
56 24 *Currently at* Department of earth Sciences, Stellenbosch University, Stellenbosch,7600,  
57 South Africa.  
58 25 *Currently at* Division of Marine Science, University of Southern Mississippi, 1020 Balch Blvd.  
59 Stennis Space Center, MS 39529, USA  
60 26 Sorbonne Universités, UPMC Univ Paris 06, CNRS, Laboratoire d'Océanographie de  
61 Villefranche (LOV), 06230 Villefranche-sur-Mer, France  
62 27 *Currently at* Earth, Ocean and Atmospheric Science, Florida State University, Tallahassee,  
63 Florida 32306, USA  
64 28 School of Earth and Environmental Sciences, Queens College, City University of New York,  
65 Flushing, USA  
66 29 Earth and Environmental Sciences, the Graduate Center, City University of New York, New  
67 York, USA  
68 30 Antarctic Climate and Ecosystem Cooperative Research Centre (ACE CRC), University of  
69 Tasmania, Private Bag 80, Hobart, TAS 7001, Australia  
70 31 Institute for Marine and Antarctic Studies, University of Tasmania, Hobart, TAS 7001,  
71 Australia

72

73

74

## 75 **Abstract**

76 The GEOVIDE cruise, a collaborative project within the framework of the international  
77 GEOTRACES programme, was conducted along the French-led section in the North Atlantic  
78 Ocean (Section GA01), between 15 May and 30 June 2014. In this Special Issue, results from  
79 GEOVIDE, including physical oceanography and trace element and isotope cyclings, are  
80 presented among seventeen articles. Here, the scientific context, project objectives and  
81 scientific strategy of GEOVIDE are provided, along with an overview of the main results from  
82 the articles published in the special issue.

83

84

## 1. Scientific context and objectives

Understanding the distribution, sources, and sinks of trace elements and isotopes (TEIs) will improve our ability to understand the past and present marine environments. Some TEIs are toxic (e.g. Hg), while others are essential micronutrients involved in many metabolic processes of marine organisms (e.g. Fe, Mn). The availability of TEIs therefore constrains the ocean carbon cycle and affects a range of other biogeochemical processes in the Earth system, whilst responding to and influencing global change (de Baar et al., 2005; Blain et al., 2007; Boyd et al., 2007; Pollard et al., 2007). Moreover, TEI interactions with the marine food web strongly depend on their physical (particulate/dissolved/colloidal/soluble) and chemical (organic and redox) forms. In addition, some TEIs are diagnostic in allowing the quantification of specific mechanisms in the marine environment that are challenging to measure directly. Few examples include: (i) atmospheric deposition (e.g.  $^{210}\text{Pb}$ , Al, Mn, Th isotopes,  $^7\text{Be}$ ; Baker et al., 2016; Hsieh et al., 2011; Measures and Brown, 1996), (ii) mixing rates of deep waters or shelf-to-open ocean (e.g.  $^{231}\text{Pa}/^{230}\text{Th}$ ,  $\Delta^{14}\text{C}$ , Ra isotopes,  $^{129}\text{I}$ ,  $^{236}\text{U}$ ; van Beek et al., 2008; Casacuberta et al., 2016; Key et al., 2004), (iii) boundary exchange processes (e.g.  $\epsilon_{\text{Nd}}$ , Jeandel et al., 2011; Lacan and Jeandel, 2001, 2005), and (iv) downward flux of organic carbon and/or remineralisation in deep waters (e.g.  $^{234}\text{Th}/^{238}\text{U}$ ,  $^{210}\text{Pb}/^{210}\text{Po}$ ,  $\text{Ba}_{\text{xs}}$ ; Buesseler et al., 2004; Dehairs et al., 1997; Roca-Martí et al., 2016). In such settings, TEIs provide chemical constraints and allow the estimation of fluxes which was not possible before the development of their analyses. Finally, paleoceanographers are wholly dependent on the development of tracers, many of which are based on TEIs used as proxies, in order to reconstruct past environmental conditions (e.g. ocean productivity, patterns and rates of ocean circulation, ecosystem structures, ocean anoxia; Henderson, 2002). Such reconstruction efforts are essential to assess the processes involved in regulating the global climate system, and possible future climate change variability.

Despite all these major implications, the distribution, sources, sinks, and internal cycling of TEIs in the oceans are still largely unknown due to the lack of appropriate clean sampling approaches and insufficient sensitivity and selectivity of the analytical measurement techniques until recently. This last point has improved very quickly as significant improvements in the instrumental techniques now allow the measurements of concentrations, speciation (physical and chemical forms), and isotopic compositions for most

117 of the elements of the periodic table which have been identified either as relevant tracers or  
118 key nutrients in the marine environment. These recent advances provide the marine  
119 geochemistry community with a significant opportunity to make substantial contributions to  
120 a better understanding of the marine environment.

121  
122 In this general context, the aim of the international GEOTRACES programme is to  
123 characterize TEI distributions on a global scale, consisting of ocean sections, and regional  
124 process studies, using a multi-proxy approach. The GEOVIDE section is the French contribution  
125 to this global survey in the North Atlantic Ocean along the OVIDE section and in the Labrador  
126 Sea (Fig. 1) and complements a range of other international cruises in the North Atlantic.  
127 GEOVIDE leans on the knowledge gained by the OVIDE project during which the Portugal-  
128 Greenland section has been carried out biennially since 2002, gathering physical and  
129 biogeochemical data from surface to bottom (Mercier et al., 2015; Pérez et al., 2018).

130

131

132 Rationale for the GEOVIDE section:

133 i) The North Atlantic Ocean plays a key role in mediating the climate of the Earth. It  
134 represents a key region of the Meridional Overturning Circulation (MOC) and a major sink of  
135 anthropogenic carbon ( $C_{\text{ant}}$ ) (Pérez et al., 2013; Sabine et al., 2004; Seager et al., 2002). Since  
136 2002, the OVIDE project has contributed to the observation of both the circulation and water  
137 mass properties of the North Atlantic Ocean. Despite the importance of the MOC on global  
138 climate, it is still challenging to assess its strength within a reasonable uncertainty (Kanzow et  
139 al., 2010; Lherminier et al., 2010). The MOC strength estimated from *in-situ* measurements on  
140 OVIDE cruises has thus helped to validate a time series for the amplitude of the MOC (based  
141 on altimetry and ARGO float array data) that exhibits a drop of  $2.5 \pm 1.4$  Sv (95% confidence  
142 interval) between 1993 and 2010 (Mercier et al., 2015), consistent with other modelling  
143 studies (Xu et al., 2013). This time series, along with the *in situ* data, shows a recovery of the  
144 MOC amplitude in 2014 at a value similar to those of the mid-1990s, confirming the  
145 importance of the decadal variability in the subpolar gyre. During OVIDE, the contribution of  
146 the most relevant currents, water masses and biogeochemical provinces have been localized  
147 and quantified. This knowledge was crucial for the establishment of the best strategy to  
148 sample TEIs in this specific region.

149 In addition to the OVIDE section, the Labrador Sea section offered a unique opportunity to  
150 complement the MOC estimate, to analyse the propagation of anomalies in temperature and  
151 salinity (Reverdin et al., 1994), and to study the distribution of TEIs along the boundary current  
152 of the subpolar gyre, coupling both observations and modelling.

153 Moreover, recent results provided evidences that CO<sub>2</sub> uptake in the North Atlantic was  
154 reduced by the weakening of the MOC (Pérez et al., 2013). The most significant finding of this  
155 study was that the uptake of C<sub>ant</sub> occurred almost exclusively in the subtropical gyre, while  
156 natural CO<sub>2</sub> uptake dominated in the subpolar gyre. In light of these new results, one issue to  
157 be addressed was the coupling between the C<sub>ant</sub> and the transport of water, with the aim to  
158 understand how the changes in the ventilation and in the circulation of water masses affect  
159 the C<sub>ant</sub> uptake and its storage capacity in the various identified provinces (Fröb et al., 2018).

160 Finally, as the subpolar North Atlantic forms the starting point for the global ocean conveyor  
161 belt, it is of particular interest to investigate how TEIs are transferred to the deep ocean  
162 through both ventilation and particle sinking, and how deep convection processes impact the  
163 TEI distributions in this key region.

164

165 ii) A better assessment of the factors that control organic production and export of carbon  
166 in the productive North Atlantic Ocean, together with a better understanding of the role  
167 played by TEIs in these processes are research priorities. Pronounced phytoplankton blooms  
168 occur in the North Atlantic in spring in response to upwelling and water column  
169 destratification (Bury et al., 2001; Henson et al., 2009; Savidge et al., 1995). Such blooms are  
170 known to trigger substantial export of fast-sinking particles (Lampitt, 1985), and can represent  
171 a major removal mechanism for particulate organic carbon, macronutrients, and TEIs to the  
172 deep ocean.

173

174 iii) In the North Atlantic, TEI distributions are influenced by a variety of sources including, for  
175 the most important, the atmosphere and the margins (Iberian, Greenland, and Labrador  
176 margins).

177

178 *Atmosphere:* Atmospheric inputs (e.g. mineral dust, anthropogenic emission aerosols) are an  
179 important sources of TEIs to the North Atlantic Ocean due to the combined effects of  
180 anthropogenic emissions from industrial/agricultural sources and mineral dust mobilized from

181 the arid regions of North Africa (Duce et al., 2008; Jickells et al., 2005). Model and satellite  
182 data for the GEOVIDE section suggested that an approximately tenfold decrease in the  
183 atmospheric concentrations of mineral dust was expected from south to north (Mahowald et  
184 al., 2005). As there had been relatively few aerosol TEI studies in the northern North Atlantic  
185 compared to the tropical and subtropical North Atlantic prior to GEOVIDE, constraining  
186 atmospheric deposition fluxes to this region had been identified as a research priority (de  
187 Leeuw et al., 2014). During the GEOVIDE campaign, a multi-proxy approach (e.g. aerosol trace  
188 element concentrations, dissolved and particulate Al and Mn, seawater  $^{210}\text{Pb}$ , Fe, Nd and Th  
189 isotopes,  $^7\text{Be}$ ) was taken to achieve the objective of better constraining the atmospheric  
190 deposition fluxes of key trace elements.

191  
192 *Margins:* The continental shelves can act as a filter for TEIs supplied from shelf sediments,  
193 submarine groundwater discharge (including the discharge of fresh groundwater into the  
194 coastal seas and recirculation of seawater through the sediment), and rivers. While some TEIs  
195 are removed on the continental shelves, others are thought to be mobilized from the solid  
196 phase at the land-ocean interface (e.g. Fe and likely other micro- and macro-nutrients, such  
197 as Cu, Ni, Mn, and Si; Chase et al., 2005; Jeandel and Oelkers, 2015). The cruise track  
198 intersected several margins, thus allowing for the characterization of continental sources and  
199 quantification of TEI fluxes associated with these sources in various shelf regimes.

200  
201 iv) It is obviously needed to further validate the use of paleo-proxies. For example, in recent  
202 years, the potential of the  $^{231}\text{Pa}/^{230}\text{Th}$  ratio for identifying past rates of ocean circulation, and  
203 of the isotopic composition of neodymium ( $\epsilon_{\text{Nd}}$ ) as a tracer of thermohaline circulation have  
204 led to many paradigm-changing results for the reconstitution of the Atlantic Ocean circulation  
205 (McManus et al., 2004; Montero-Serrano et al., 2013; Negre et al., 2010). However, there is  
206 an ongoing debate about the interpretation of  $^{231}\text{Pa}/^{230}\text{Th}$  paleo-records in the Atlantic (Hayes  
207 et al., 2015; Keigwin and Boyle, 2008) focused on the effects of particle fluxes versus those of  
208 water circulation. Only one single  $^{231}\text{Pa}$  profile in the Subpolar North Atlantic has been  
209 published before GEOVIDE (Moran et al., 2002). Regarding Nd isotopes, although several  
210 profiles of dissolved (and total) Nd isotopes are available in the boundary currents of  
211 Greenland and the Labrador Sea, there are very few profiles for the ocean interior of the  
212 GEOVIDE region (Copard et al., 2011; Filippova et al., 2017; Lacan and Jeandel, 2004; Lambelet

213 et al., 2016). In addition, the importance of dissolved/particle interactions in the control of  
214 the isotopic composition of Nd is becoming increasingly apparent. To our knowledge,  
215 particulate  $\epsilon_{Nd}$  data have not been published yet for the Subpolar North Atlantic. For these  
216 reasons, documenting these tracers in both dissolved and particulate phases is needed to  
217 provide new constraints and significantly advance our understanding of the cycles of these  
218 tracers and their use in the modern and past oceans.

219 Furthermore, proxies of nutrient utilization, such as the silicon stable isotopes ( $\delta^{30}Si$ ) from  
220 diatom silica, provides a means of reconstructing the behaviour of past geochemical cycles  
221 and the past strength of the biological pump, and its influence on atmospheric concentrations  
222 of  $CO_2$ . However, successful application of  $\delta^{30}Si$  in diatoms accumulating in sediments for  
223 reconstruction of past silica cycling requires a thorough understanding of  $\delta^{30}Si$  of dissolved Si  
224 ( $\delta^{30}Si_{DSi}$ ) and of the processes that control its distribution throughout the modern ocean.  
225 Combining studies in the Southern Ocean (De La Rocha et al., 2011; Fripiat et al., 2011) and  
226 North and Equatorial Pacific (De La Rocha et al., 2000) with a global circulation model  
227 (Wischmeyer et al., 2003) has revealed the roles that ocean circulation and biogeochemical  
228 cycling play in controlling the distribution of silicon isotopes within the ocean. Largely missing  
229 from this dataset was the North Atlantic Ocean (De La Rocha et al., 2011).

230  
231 In this general context, the main scientific objectives of GEOVIDE were to (i) better  
232 understand and quantify the MOC and the carbon cycle carbon cycle in the context of decadal  
233 variability, adding new tracers to this end, (ii) map the TEI distributions, including their physical  
234 and chemical speciation, along this full-depth high resolution ocean section, (iii) investigate  
235 the links between TEIs and the production, export, and remineralisation of particulate organic  
236 matter, (iv) identify TEI sources and sinks, and quantify their fluxes at the ocean boundaries,  
237 and (v) better understand and quantify the paleoproxies  $^{231}Pa/^{230}Th$ ,  $\epsilon_{Nd}$ , and  $\delta^{30}Si$ .

238

239

## 240 2. Strategy

241

242 To achieve the objectives of the GEOVIDE project, a 47-day multidisciplinary cruise was  
243 carried out on board R/V Pourquoi Pas? in the North Atlantic Ocean along the OVIDE section,  
244 from Lisbon to Greenland, and in the Labrador Sea (Fig. 1). The Labrador section was chosen

245 according to the OSNAP (Overturning in the Subpolar North Atlantic Programme)  
246 recommendations because it transects the export route of the Labrador Sea Water  
247 downstream of its formation site. Therefore, the properties of the North Atlantic Deep Water  
248 (NADW) at 53°N are likely to be representative of NADW further south and a 15-year time  
249 series of currents and hydrographic properties is available in the Western Boundary Current  
250 at this latitude (Fischer et al., 2010). The GEOVIDE cruise took place from 15 May to 30 June  
251 2014, during the same season as the previous OVIDE cruises (2002-2012). The cruise timing  
252 helped to minimize seasonal variations and maximize the representativeness of inter-annual  
253 variability of the physical parameters investigated in this specific region. Furthermore, this  
254 period of the year corresponds to the bloom/post-bloom period of the subpolar gyre and post-  
255 bloom period in the sub-tropical gyre (Henson et al., 2005), thus allowing for the study of the  
256 complexity of the biological pump and the links between production, export of organic matter,  
257 and TEIs.

258 A high resolution hydrographical section that includes the *in-situ* measurements of the  
259 currents by doppler profilers was performed and, as recommended by GEOTRACES, a multi-  
260 proxy approach was used. In total, 78 stations were occupied (plus one test station). Station  
261 naming depended on the number of casts that were conducted: Short (47 one-cast stations),  
262 Large (17 three-cast stations), XLarge (5 five-cast stations), and Super (10 multi-cast stations).  
263 A total of 341 on-deck operations were carried out during GEOVIDE.

264 In total, (i) the standard stainless steel rosette was deployed 163 times, (ii) the trace metal  
265 clean rosette, 53 times, (iii) *in-situ* pumps, 25 times, (iv) the mono-corer, with or without *in-*  
266 *situ* pumps clamped on the cable, 11 times and (v) the plankton net, 9 times. We also collected  
267 140 surface seawater samples using a fish towed from the ship's starboard side and deployed  
268 at 1–2 m depth, 18 aerosol samples, and 10 rainwater samples. In addition, we deployed: 60  
269 eXpendable BathyThermographs (XBTs), 17 ARGO profiling floats (8 ARVOR, 2 ARVOR-deep, 2  
270 PROVOR-DO, 2 PROVBIO, 1 ARVOR double DO, and 2 APEX), and 12 weather buoys.

271

272

### 273 3. Summary of the main results published in this special issue

274

275 In this special issue, seventeen publications present results of the GEOVIDE project. Six other  
276 manuscripts have already been published in other journals (Benetti et al., 2017; Cossa et al.,



277 2018b; Le Reste et al., 2016; Pérez et al., 2018; Shelley et al., 2017; Zunino et al., 2015). Due  
278 to the long time required for some analyses, other articles related to this project are to be  
279 expected for publication at a later date.

280 The articles in this special issue are linked to four general research themes: (i) hydrographic  
281 and physical characteristics, (ii) links between water masses and TEIs, (iii) external sources and  
282 sinks of TEIs, and (iv) biogeochemical tracers of community structure, export and  
283 remineralisation.

284

### 285 3.1. Hydrographic and physical characteristics

286 In terms of circulation, the comparison with the 2002–2012 mean state shows a different  
287 repartition of the northward warm currents that compose the upper limb of the MOC, with a  
288 more intense Irminger Current (station 39-41) and a weaker North Atlantic Current (NAC) in  
289 the Western European Basin, these anomalies being compatible with the variability previously  
290 observed along the OVIDE section in the 2000s (Zunino et al., 2017). The distribution of the  
291 volume transport in the three branches of the NAC (Fig. 1) has changed: no transport was  
292 found in the northern branch, although 11 Sv were found in the mean of the previous decade,  
293 and the central branch, that marks the limit between the subpolar and the subtropical regions,  
294 nearly doubled in 2014.

295 The main hydrographic properties along the GEOVIDE section are shown on Fig. 2 for  
296 potential temperature, salinity, dissolved oxygen, nitrate + nitrite, and silicic acid. The surface  
297 waters of the eastern SPNA, down to about 500 m, were much colder and fresher than the  
298 average values observed over 2002–2012 (Zunino et al., 2017). In the context of the ocean  
299 heat loss observed in the subpolar gyre since 2005, the year 2013-2014 was indeed particularly  
300 intense. Remarkably, despite the negative temperature anomalies in the surface waters, the  
301 heat transport across the OVIDE section estimated during GEOVIDE was the largest measured  
302 since 2002. This was attributed to the relatively strong MOC measured across the OVIDE  
303 section during GEOVIDE (Zunino et al., 2017) and more particularly to the strong transport of  
304 central water in the central and southern branch of the NAC (García-Ibáñez et al., 2018) that  
305 compensates the cold anomaly of the surface layer. The relatively strong MOC and heat  
306 transport were confirmed by Holliday et al. (2018) across a nearly simultaneous section (June-  
307 July 2014) between Labrador and Scotland.

308 The water mass properties of the GEOVIDE cruise were used to perform an extended  
309 Optimum MultiParameter (eOMP) analysis and to assess the water mass distribution (García-  
310 Ibáñez et al., 2018). The eOMP analysis together with the absolute geostrophic velocity field  
311 determined using a box inverse model allowed the evaluation of the relative importance of  
312 each water mass to the MOC. The increase in the MOC intensity from 2002–2010 to 2014 was  
313 shown to be related to the increase in the northward transport of the Central Waters in its  
314 upper limb (from the surface to 1000 m in the south-eastern part of the section), and in the  
315 southward flow of both the Subpolar Mode Water of the Irminger Basin (SPMW, 200 to  
316 1500 m) and the Iceland–Scotland Overflow Water (ISOW, between 1800 and 3000 m) in its  
317 lower limb (García-Ibáñez et al., 2018).

318 In addition, the precise determination of different water masses (García-Ibáñez et al., 2018)  
319 and ventilation processes are crucial for the interpretation of the TEIs whose distributions are,  
320 for many of them, strongly related to water masses.

321

### 322 3.2. Links between water masses and TEIs

323 The concentrations of TEIs are strongly influenced by water mass distribution, age, and  
324 circulation/mixing. For instance, this is the case of  $^{230}\text{Th}$  and  $^{231}\text{Pa}$ , high concentrations of both  
325 tracers were observed in the old water of North East Atlantic Deep Water (NEADW), and low  
326 values in young waters, particularly in Denmark Strait Overflow Water (DSOW) (Deng et al.,  
327 2018). The low values of  $^{230}\text{Th}$  and  $^{231}\text{Pa}$  in water near the seafloor of the Labrador and  
328 Irminger Seas are related to the young waters present in those regions (Deng et al., 2018).  
329 This study reports systematic increase of  $^{230}\text{Th}$  activities with water age but a more complex  
330 relationship between age and  $^{231}\text{Pa}$  which challenges some approaches to the use of  
331 sedimentary  $^{231}\text{Pa}/^{230}\text{Th}$  ratios to assess past rates of oceanic circulation. The application of  
332 this proxy at a basin scale to constrain the overturning circulation is, however, supported by  
333 GEOVIDE data which now allows a complete nuclide budget for the North Atlantic to be  
334 constructed (Deng et al., 2018).

335 Long-lived artificial radionuclides were also very useful to assess the circulation in the  
336 SPNA, namely  $^{129}\text{I}$  and  $^{236}\text{U}$ , and the origin of water masses in a dual tracer approach (i.e.  
337  $^{129}\text{I}/^{236}\text{U}$  and  $^{236}\text{U}/^{238}\text{U}$  atom ratios) (Castrillejo et al., 2018). These transient tracers, originating  
338 from La Hague (France) and Sellafield (UK) nuclear reprocessing plants and the atmospheric  
339 nuclear weapon tests, helped investigating the shallow western boundary transport and the

340 ventilation processes. For example, the  $^{129}\text{I}$  concentrations validate the ISOW transport  
341 pathways in the Western European basin. The time series of  $^{129}\text{I}$  in the Labrador Sea revealed  
342 two circulation loops of the Atlantic Waters carrying the signal from the European  
343 reprocessing plants: i) a short loop through the Nordic Seas into the central Labrador Sea of  
344 about 8-10 years, and; ii) a longer loop which includes about 8 additional years of recirculation  
345 in the Arctic Eurasian Basin before entering back to the Atlantic Ocean (Castrillejo et al., 2018).

346 Some other TEIs were also strongly linked to water mass distribution: Within GEOVIDE,  
347 silicon isotopes (Sutton et al., 2018), lead (Pb) (Zurbrick et al., 2018), mercury (Hg) (Cossa et  
348 al., 2018a), and particulate and dissolved Fe and Al (Gourain et al., 2018; Menzel Barraqueta  
349 et al., 2018a; Tonnard et al., 2018), as examples. For instance, the Labrador Seawater (LSW) is  
350 characterized by a relatively high silicon stable isotope composition for dissolved silicon  
351 ( $\delta^{30}\text{Si}_{\text{DSi}}$ ) whose signature can be seen not only in the region where it is formed, but also  
352 throughout the mid-depth zone of the North Atlantic Ocean (Sutton et al., 2018). The  $\delta^{30}\text{Si}_{\text{DSi}}$   
353 distribution thus provides information on the interaction between subpolar/polar water  
354 masses of northern and southern origin, and indicates the extent to which local signatures are  
355 influenced by source waters (Sutton et al., 2018). In LSW, the concentrations of Pb (Zurbrick  
356 et al., 2018) and Hg (Cossa et al., 2018a) provided evidence for a decrease in the  
357 anthropogenic inputs of these two elements over the last decade, since the values are lower  
358 in the recently formed LSW between Greenland and Newfoundland than in the older LSW of  
359 the Western European basin.

360 The Mediterranean Water (MW), meanwhile, was characterised by higher concentrations  
361 of trace metals, such as Pb, Hg, and Al (Cossa et al., 2018a; Menzel Barraqueta et al., 2018a;  
362 Zurbrick et al., 2018). It reflects the importance of Saharan and anthropogenic atmospheric  
363 inputs to the Mediterranean region, which are much higher than in our studied area (see  
364 below), as well as enhanced remineralisation as indicated by the correlation between total  
365 mercury concentrations and the apparent oxygen utilisation (Cossa et al., 2018a).

366

### 367 3.3. TEI sources and sinks

368 Different methods/TEIs were used to estimate atmospheric input fluxes: aerosol  
369 concentrations in aerosol and rainwater samples were compared with estimates derived from  
370 the measurement of beryllium-7 ( $^7\text{Be}$ ) in aerosols, rainwater and seawater (Shelley et al.,  
371 2017). Taking a different approach, Menzel Barraqueta et al. (2018b) used dAl in the surface

372 waters to estimate the atmospheric input flux. All these methods allowed concluding that the  
373 atmospheric inputs of total trace elements were low in our study area, and the soluble input  
374 was even lower, based on their fractional solubility (Shelley et al., 2018).

375 One of the main sources of TEIs during GEOVIDE was sediment input (i) within the benthic  
376 nepheloid layers in the Iceland, Irminger and Labrador Basins (Gourain et al., 2018), and (ii)  
377 above the Iberian, Greenland and Canadian margins, as well as fluvial and meteoric inputs  
378 (Benetti et al., 2017). This is notably the case for some dissolved TEIs, such as Fe (Tonnard et  
379 al., 2018), Al (Menzel Barraqueta et al., 2018a), and radium-226 ( $^{226}\text{Ra}$ ) or barium (Ba) (Le Roy  
380 et al., 2018), as well as for particulate trace elements (Gourain et al., 2018). Overall, enhanced  
381 concentrations of TEIs close to the bottom suggest that continental shelves and margins acted  
382 as a source to adjacent waters. In the case of the Iberian margin, advection of particulate Fe  
383 (pFe) was visible over a distance of more than 250 km from the source (Gourain et al., 2018).

384 However, some results provide evidence that occasional removal of dFe or dAl by particles  
385 can be a dominant process rather than partial dissolution from resuspended sediments, but  
386 this is likely dependent on the nature of particles (Menzel Barraqueta et al., 2018a).

387 Additional sources for particulate elements and sinks for dissolved ones are biological  
388 uptake and scavenging. Evidence for a biogenic influence on the pFe/pAl ratios within the  
389 Irminger and Labrador Basins was found by Gourain et al. (2018). Almost all the stations  
390 displayed dFe minima in surface waters, in association with the chlorophyll maxima. The  
391 abundance of diatoms exerted a significant control on the surface concentrations of Fe and Al  
392 (Menzel Barraqueta et al., 2018b; Tonnard et al., 2018). Remineralisation processes were also  
393 highlighted for some TEIs (see also section 3.4). Dissolved Al concentrations generally  
394 increased with depth and the net release of dAl at depth during remineralisation of sinking  
395 biogenic opal containing particles was generally larger than the net removal of dAl through  
396 scavenging.

397

#### 398 3.4. Production, export, and remineralisation

399 The main biogeochemical features of the GEOVIDE cruise in terms of biogenic silica (BSi),  
400 particulate organic carbon (POC), and particulate organic nitrogen (PON) are reported on Fig.  
401 3 and supplementary material. The higher BSi concentrations were observed in the Irminger  
402 and Labrador Seas. POC and PON were also high in these regions, but also show high values in  
403 the Iceland and Western European Basins.

404 On the Iberian margin and in the Western European Basin, an unexpectedly high  
405 heterotrophic nitrogen fixation activity was reported, likely sustained by the availability of  
406 phytoplankton-derived organic matter (dissolved and/or particulate), resulting from the on-  
407 going to post spring bloom conditions, while dissolved iron supply relied on atmospheric  
408 deposition and surface waters advection from the subtropical region and the shelf area  
409 (Fonseca-Batista et al., 2018).

410 In terms of particulate organic carbon (POC) export, thorium-234 ( $^{234}\text{Th}$ ) was used to  
411 provide estimates of POC export fluxes, with the highest values near the Iberian margin where  
412 a phytoplankton bloom was declining, and the lowest values in the Irminger Basin where the  
413 bloom was close to its maximum (Lemaitre et al., 2018a). The proxy  $^{210}\text{Po}/^{210}\text{Pb}$  was also used  
414 to assess the export of particles (Tang et al., 2018). The prominent role of small particles in  
415 sorption was confirmed, suggesting that particulate radionuclide activities and export of both  
416 small (1-53  $\mu\text{m}$ ) and large (> 53  $\mu\text{m}$ ) particles should be considered to account for the observed  
417 surface water  $^{210}\text{Po}/^{210}\text{Pb}$  disequilibria (Tang et al., 2018).

418 In the subpolar and subtropical regions, the mesopelagic POC remineralisation fluxes,  
419 estimated from the particulate biogenic barium (excess barium;  $\text{Ba}_{\text{xs}}$ ) proxy, were found to be  
420 equal to and occasionally higher than the upper ocean POC export fluxes (Lemaitre et al.,  
421 2018b). These results highlighted the strong impact of the mesopelagic remineralisation on  
422 the biological carbon pump with a very low carbon sequestration efficiency at the time of our  
423 study (Lemaitre et al., 2018b).

424

425

## 426 **Conclusion**

427 The main GEOVIDE results have helped to improve our understanding of the TEI cycles in the  
428 North Atlantic. The strong physical oceanography background of the GEOVIDE project is a  
429 strength for interpreting our data. For many TEIs, a strong link was observed between their  
430 distributions and water masses. On the other hand, TEIs also helped to constrain oceanic  
431 circulation, notably in the subpolar gyre and Labrador Sea. Important sources (sediments,  
432 fluvial, and meteoric) and sinks (biological uptake and scavenging) of TEIs were highlighted.  
433 The biological carbon pump was studied and showed different efficiencies in the various  
434 studied regions.

435

436 **Acknowledgements:**

437 We are greatly thankful to the captain, Gilles Ferrand, and crew of the N/O Pourquoi Pas?  
438 for their help during the GEOVIDE mission. This work was supported by the French National  
439 Research Agency (ANR-13-BS06-0014, ANR-12-PDOC-0025-01), the French National Centre for  
440 Scientific Research (CNRS-LEFE-CYBER), the LabexMER (ANR-10-LABX-19), and Ifremer. It was  
441 supported for the logistic by DT-INSU and GENAVIR.

442

443 **References**

- 444 de Baar, H. J. W., Boyd, P. X., Coale, K. H., Landry, M. R., Tsuda, A., Assmy, P., Bakker, D. C. E., Bozec,  
445 Y., Barber, R. T., Brzezinski, M. A., Buesseler, K. O., Boye, M., Croot, P. L., Gervais, F., Gorbunov,  
446 M. Y., Harrison, P. J., Hiscock, W. T., Laan, P., Lancelot, C., Law, C. S., Lvasseur, M., Marchetti, A.,  
447 Millero, F., Nishioka, J., Nojiri, Y., van Oijen, T., Riebesell, U., Rijkenberg, M. J. A., Saito, H., Takeda,  
448 S., Timmermans, K. R., Veldhuis, M. J. W., Waite, A. M. and Wong, C.-S.: Synthesis of iron  
449 fertilization experiments: From the Iron Age in the Age of Enlightenment, *J Geophys Res*, 110,  
450 C09S16, doi:10.1029/2004JC002601, 2005.
- 451 Baker, A. R., Landing, W. F., Bucciarelli, E., Cheize, M., Fietz, S., Hayes, C. T., Kadko, D., Morton, P. L.,  
452 Rogan, N., Sarthou, G., Shelley, R. U., Shi, Z., Shiller, A. M. and Van Hulten, M. M. P.: Air - Sea  
453 Deposition of Trace Elements | *Philosophical Transactions of the Royal Society of London A:*  
454 *Mathematical, Physical and Engineering Sciences*, [online] Available from:  
455 <http://rsta.royalsocietypublishing.org/content/374/2081/20160190> (Accessed 18 June 2018),  
456 2016.
- 457 van Beek, P., Bourquin, M., J.-L., R., Souhaut, M., Charette, M. A. and Jeandel, C.: Radium isotopes to  
458 investigate the water mass pathways on the Kerguelen Plateau (Southern Ocean), *Deep Sea Res*  
459 *II*, 55(5–7), 622–637, 2008.
- 460 Benetti, M., Reverdin, G., Lique, C., Yashayaev, I., Holliday, N. P., Tynan, E., Torres-Valdes, S.,  
461 Lherminier, P., Tréguer, P. and Sarthou, G.: Composition of freshwater in the spring of 2014 on  
462 the southern Labrador shelf and slope, *J. Geophys. Res. Oceans*, 122(2), 1102–1121,  
463 doi:10.1002/2016JC012244, 2017.
- 464 Blain, S., Quéguiner, B., Armand, L., Belviso, S., Bombled, B., Bopp, L., Bowie, A., Brunet, C., Brussaard,  
465 C., Carlotti, F., Christaki, U., Corbière, A., Durand, I., Ebersbach, F., Fuda, J.-L., Garcia, N., Gerringa,  
466 L., Griffiths, B., Guigue, C., Guillerm, C., Jacquet, S., Jeandel, C., Laan, P., Lefèvre, D., Lomonaco,  
467 C., Malits, A., Mosseri, J., Obernosterer, I., Park, Y.-H., Picheral, M., Pondaven, P., Remenyi, T.,  
468 Sandroni, V., Sarthou, G., Savoye, N., Scouarnec, L., Souhaut, M., Thuiller, D., Timmermans, K.,  
469 Trull, T., Uitz, J., van-Beek, P., Veldhuis, M., Vincent, D., Viollier, E., Vong, L. and Wagener, T.:  
470 Impact of natural iron fertilization on carbon sequestration in the Southern Ocean, *Nature*, 7139,  
471 1070–1074, 2007.
- 472 Boyd, P. W., Jickells, T., Law, C. S., Blain, S., Boyle, E. A., Buesseler, K. O., Coale, K. H., Cullen, J. J., Baar,  
473 H. J. W. de, Follows, M., Harvey, M., Lancelot, C., Lvasseur, M., Owens, N. P. J., Pollard, R., Rivkin,  
474 R. B., Sarmiento, J., Schoemann, V., Smetacek, V., Takeda, S., Tsuda, A., Turner, S. and Watson, A.  
475 J.: Mesoscale Iron Enrichment Experiments 1993–2005: Synthesis and Future Directions, *Science*,  
476 315, 612–617, 2007.
- 477 Buesseler, K. O., Andrews, J. E., Pike, S. M. and Charette, M. A.: The effects of iron fertilization on  
478 carbon sequestration in the Southern Ocean, *Science*, 304(5669), 414–417, 2004.
- 479 Bury, S. J., Boyd, P. W., Preston, T., Savidge, G. and Owens, N. J. P.: Size-fractionated primary  
480 production and nitrogen uptake during a North Atlantic phytoplankton bloom : implications for  
481 carbon export estimates, *Deep Sea Res. Part 1 Oceanogr. Res. Pap.*, 48(3), 689–720; 7, 2001.

482 Casacuberta, N., Masqué, P., Henderson, G., Rutgers van-der-Loeff, M., Bauch, D., Vockenhuber, C.,  
483 Daraoui, A., Walther, C., Synal, H.-A. and Christl, M.: First  $^{236}\text{U}$  data from the Arctic Ocean and  
484 use of  $^{236}\text{U}/^{238}\text{U}$  and  $^{129}\text{I}/^{236}\text{U}$  as a new dual tracer, *Earth Planet. Sci. Lett.*, 440, 127–134,  
485 doi:10.1016/j.epsl.2016.02.020, 2016.

486 Castrillejo, M., Casacuberta, N., Christl, M., Vockenhuber, C., Synal, H.-A., García-Ibáñez, M. I.,  
487 Lherminier, P., Sarthou, G., Garcia-Orellana, J. and Masqué, P.: Tracing water masses with  $^{129}\text{I}$  and  
488  $^{236}\text{U}$  in the subpolar North Atlantic along the GEOTRACES GA01 section, *Biogeosciences*, 15(18),  
489 5545–5564, doi:https://doi.org/10.5194/bg-15-5545-2018, 2018.

490 Chase, Z., Johnson, K. S., Elrod, V. A., Plant, J. N., Fitzwater, S. E., Pickella, L. and Sakamoto, C. M.:  
491 Manganese and iron distributions off central California influenced by upwelling and shelf width,  
492 *Mar Chem*, 95, 235–254, 2005.

493 Copard, K., Colin, C., Frank, N., Jeandel, C., Montero-Serrano, J. C., Reverdin, G. and Ferron, B.: Nd  
494 isotopic composition of water masses and dilution of the Mediterranean outflow along the  
495 southwest European margin, *Geochem Geophys Geosyst*, 12, Q06020, 10.1029/2011GC003529,  
496 2011.

497 Cossa, D., Heimbürger, L.-E., Pérez, F. F., García-Ibáñez, M. I., Sonke, J. E., Planquette, H., Lherminier,  
498 P., Boutorh, J., Cheize, M., Menzel Barraqueta, J. L., Shelley, R. and Sarthou, G.: Mercury  
499 distribution and transport in the North Atlantic Ocean along the GEOTRACES-GA01 transect,  
500 *Biogeosciences*, 15(8), 2309–2323, doi:10.5194/bg-15-2309-2018, 2018a.

501 Cossa, D., Heimbürger, L. E., Sonke, J. E., Planquette, H., Lherminier, P., García-Ibáñez, M. I., Pérez, F.  
502 F. and Sarthou, G.: Sources, cycling and transfer of mercury in the Labrador Sea (Geotraces-  
503 Geovide cruise), *Mar. Chem.*, 198, 64–69, doi:10.1016/j.marchem.2017.11.006, 2018b.

504 Daniault, N., Mercier, H., Lherminier, P., Sarafanov, A., Falina, A., Zunino, P., Pérez, F. F., Ríos, A. F.,  
505 Ferron, B., Huck, T., Thierry, V. and Gladyshev, S.: The northern North Atlantic Ocean mean  
506 circulation in the early 21st century, *Prog. Oceanogr.*, 146, 142–158,  
507 doi:10.1016/j.pocean.2016.06.007, 2016.

508 De La Rocha, C. L., Hutchins, D. A., Brzezinski, M. A. and Zhang, Y.: Effects of iron and zinc deficiency  
509 on elemental composition and silica production by diatoms, *Mar Ecol Progr Ser*, 195, 71–79, 2000.

510 De La Rocha, C. L., Bescont, P., Croguennoc, A. and Ponzevera, E.: The silicon isotopic composition of  
511 surface waters of the Atlantic and Indian sectors of the Southern Ocean, *Geochim. Cosmochim.*  
512 *Acta*, 75, 5283–5295, 2011.

513 Dehairs, F., Shopova, D., Ober, S., Veth, C. and Goeyens, L.: Particulate barium stocks and oxygen  
514 consumption in the Southern Ocean mesopelagic water column during spring and early summer:  
515 relationship with export production, *Deep Sea Res. Part II Top. Stud. Oceanogr.*, 44(1), 497–516,  
516 doi:10.1016/S0967-0645(96)00072-0, 1997.

517 Deng, F., Henderson, G. M., Castrillejo, M. and Perez, F. F.: Evolution of  $^{231}\text{Pa}$  and  $^{230}\text{Th}$  in overflow  
518 waters of the North Atlantic, *Biogeosciences Discuss*, 1–24, doi:10.5194/bg-2018-191, in review,  
519 2018.

520 Duce, R. A., LaRoche, J., Altieri, K., Arrigo, K. R., Baker, A. R., Capone, D. G., Cornell, S., Dentener, F.,  
521 Galloway, J., Ganeshram, R. S., Geider, R. J., Jickells, T., Kuypers, M. M., Langlois, R., Liss, P. S., Liu,  
522 S. M., Middelburg, J. J., Moore, C. M., Nickovic, S., Oschlies, A., Pedersen, T., Prospero, J., Schlitzer,  
523 R., Seitzinger, S., Sorensen, L. L., Uematsu, M., Ulloa, O., Voss, M., Ward, B. and Zamora, L.:  
524 Impacts of atmospheric anthropogenic nitrogen on the open ocean, *Science*, 320(5878), 893–897,  
525 doi:10.1126/science.1150369, 2008.

526 Filippova, A., Frank, M., Kienast, M., Rickli, J., Hathorne, E., Yashayaev, I. M. and Pahnke, K.: Water  
527 mass circulation and weathering inputs in the Labrador Sea based on coupled Hf–Nd isotope  
528 compositions and rare earth element distributions, *Geochim. Cosmochim. Acta*, 199, 164–184,  
529 doi:10.1016/j.gca.2016.11.024, 2017.

530 Fischer, J., Visbeck, M., Zantopp, R., Nunes, N. and doi.: Interannual to decadal variability of outflow  
531 from the Labrador Sea, *Geophys Res Lett*, 37, L24610, doi:10.1029/2010GL045321, 2010.

532 Fonseca-Batista, Li, X., Riou, V., Michotey, V., Fripiat, F., Deman, F., Guasco, S., Brion, N., Lemaitre, N.,  
533 Planchon, F., Tonnard, M., Planquette, H., Sarthou, G., Elskens, M., Chou, L. and Dehairs, F.:

534 Evidence of high N<sub>2</sub> fixation rates in productive waters of the temperate Northeast Atlantic,  
535 Biogeosciences Discuss, <https://doi.org/10.5194/bg-2018-220>, in review, 2018.

536 Fripiat, F., Cavagna, A.-J., Nicolas, S., Dehairs, F., Andre, L. and Cardinal, D.: Isotopic constraints on the  
537 Si-biogeochemical cycle of the Antarctic Zone in the Kerguelen area (KEOPS), *Mar Chem*, 123(1–  
538 4), 11–22, DOI: 10.1016/j.marchem.2010.08.005, 2011.

539 Fröb, F., Olsen, A., Pérez, F. F., García-Ibáñez, M. I., Jeansson, E., Omar, A. and Lauvset, S. K.: Inorganic  
540 carbon and water masses in the Irminger Sea since 1991, *Biogeosciences*, 15(1), 51–72,  
541 doi:10.5194/bg-15-51-2018, 2018.

542 García-Ibáñez, M. I., Pérez, F. F., Lherminier, P., Zunino, P., Mercier, H. and Tréguer, P.: Water mass  
543 distributions and transports for the 2014 GEOVIDE cruise in the North Atlantic, *Biogeosciences*,  
544 15(7), 2075–2090, doi:10.5194/bg-15-2075-2018, 2018.

545 Gourain, A., Planquette, H., Cheize, M., Lemaitre, N., Menzel Barraqueta, J.-L., Shelley, R., Lherminier,  
546 P. and Sarthou, G.: Inputs and processes affecting the distribution of particulate iron in the North  
547 Atlantic along the GEOVIDE (GEOTRACES GA01) section, *Biogeosciences Discuss*, 1–42,  
548 doi:10.5194/bg-2018-234, 2018.

549 Hayes, C. T., Anderson, R. F., Fleisher, M. Q., Huang, K.-F., Robinson, L. F., Lu, Y., Cheng, H., Edwards,  
550 R. L. and Moran, S. B.: 230Th and 231Pa on GEOTRACES GA03, the U.S. GEOTRACES North Atlantic  
551 transect, and implications for modern and paleoceanographic chemical fluxes, *Deep Sea Res. Part*  
552 *II Top. Stud. Oceanogr.*, 116, 29–41, doi:10.1016/j.dsr2.2014.07.007, 2015.

553 Henderson, G. M.: New oceanic proxies for paleoclimate, *Earth Planet Sci Lett*, 203, 1–13, 2002.

554 Henson, S. A., Dunne, J. P. and Sarmiento, J. L.: Decadal variability in North Atlantic phytoplankton  
555 blooms, *J Geophys Res*, 114, C04013, doi:10.1029/2008JC005139, 2009.

556 Holliday, N. P., Bacon, S., Cunningham, S. A., Gary, S. F., Karstensen, J., King, B. A., Li, F. and Mcdonagh,  
557 E. L.: Subpolar North Atlantic Overturning and Gyre-Scale Circulation in the Summers of 2014 and  
558 2016, *J. Geophys. Res. Oceans*, 123(7), 4538–4559, doi:10.1029/2018JC013841, 2018.

559 Hsieh, Y.-T., Henderson, G. M. and Thomas, A. L.: Combining seawater 232Th and 230Th concentrations  
560 to determine dust fluxes to the surface ocean, *Earth Planet Sci. Lett*, 312, 280–290,  
561 doi:10.1016/j.epsl.2011.10.022, 2011.

562 Jeandel, C. and Oelkers, E. H.: The influence of terrigenous particulate material dissolution on ocean  
563 chemistry and global element cycles, *Chem. Geol.*, 395, 50–66,  
564 doi:10.1016/j.chemgeo.2014.12.001, 2015.

565 Jeandel, C., Peucker Ehrenbrink, B., Jones, M., Pearce, C., Oelkers, E., Godderis, Y., Lacan, F., Aumont,  
566 O. and Arsouze, T.: Ocean margins: the missing term for oceanic element budgets?, *EOS*, 92, 217–  
567 219, 2011.

568 Jickells, T. D., An, Z. S., Andersen, K. K., Baker, A. R., Bergametti, G., Brooks, N., Cao, J. J., Boyd, P. W.,  
569 Duce, R. A., Hunter, K. A., Kawahata, H., Kubilay, N., La Roche, J., Liss, P. S., Mahowald, N.,  
570 Prospero, J. M., Ridgwell, A. J., Tegen, I. and Torres, R.: Global Iron Connections Between Desert  
571 Dust, Ocean Biogeochemistry, and Climate, *Science*, 308, 67–71, 2005.

572 Kanzow, T., Cunningham, S. A., Johns, W. E., Hirschi, J. J.-M., Marotzke, J., Baringer, M. O., Meinen, C.  
573 S., Chidichimo, M. P., Atkinson, C., Beal, L. M., Bryden, H. L. and Collins, J.: Seasonal Variability of  
574 the Atlantic Meridional Overturning Circulation at 26.5°N, *J Clim.*, 23, 5678–5698,  
575 doi:10.1175/2010JCLI3389.1, 2010.

576 Keigwin, L. D. and Boyle, E. A.: Did North Atlantic overturning halt 17,000 years ago?,  
577 *Paleoceanography*, 23(1), doi:10.1029/2007PA001500, 2008.

578 Key, R. M., Kozyr, A., Sabine, C. L., Lee, K., Wanninkhof, R., Bullister, J. L., Feely, R. A., Millero, F. J.,  
579 Mordy, C. and Peng, T.-H.: A global ocean carbon climatology: Results from the Global Data  
580 Analysis Project (GLODAP), *Glob. Biogeochem Cycles*, 18, 10.1029/2004GB002247, 2004.

581 Lacan, F. and Jeandel, C.: Tracing Papua New Guinea imprint on the central Equatorial Pacific Ocean  
582 using neodymium isotopic compositions and Rare Earth Element patterns, *Earth Planet Sci Lett*,  
583 5779, 1–16, 2001.

584 Lacan, F. and Jeandel, C.: Subpolar Mode Water formation traced by neodymium isotopic composition,  
585 *Geophys. Res. Lett.*, 31, L14306, doi:10.1029/2004GL019747, 2004, 2004.



586 Lacan, F. and Jeandel, C.: Neodymium isotopes as a new tool for quantifying exchange fluxes at the  
587 continent-ocean interface, *Earth Planet Sci Lett*, 232(3–4), 245–257,  
588 doi:10.1016/j.epsl.2005.01.004, 2005.

589 Lambelet, M., van de Flierdt, T., Crocket, K., Rehkämper, M., Kreissig, K., Coles, B., Rijkenberg, M. J. A.,  
590 Gerringa, L. J. A., de Baar, H. J. W. and Steinfeldt, R.: Neodymium isotopic composition and  
591 concentration in the western North Atlantic Ocean: Results from the GEOTRACES GA02 section,  
592 *Geochim. Cosmochim. Acta*, 177(Supplement C), 1–29, doi:10.1016/j.gca.2015.12.019, 2016.

593 Lampitt, R. S.: Evidence for the seasonal deposition of detritus to the deep-sea floor and its subsequent  
594 resuspension, *Deep Sea Res I*, 32(8), 885–897, 1985.

595 Le Reste, S., Dutreuil, V., André, X., Thierry, V., Renaut, C., Le Traon, P.-Y. and Maze, G.: “Deep-Arvor”:  
596 A New Profiling Float to Extend the Argo Observations Down to 4000-m Depth, *J. Atmospheric*  
597 *Ocean. Technol.*, 33(5), 1039–1055, doi:10.1175/JTECH-D-15-0214.1, 2016.

598 Le Roy, E., Sanial, V., Charette, M. A., Beek, P. van, Lacan, F., Jacquet, S. H. M., Henderson, P. B.,  
599 Souhaut, M., García-Ibáñez, M. I., Jeandel, C., Pérez, F. F. and Sarthou, G.: The <sup>226</sup>Ra–Ba  
600 relationship in the North Atlantic during GEOTRACES-GA01, *Biogeosciences*, 15(9), 3027–3048,  
601 doi:https://doi.org/10.5194/bg-15-3027-2018, 2018.

602 de Leeuw, G., Guieu, C., Arneth, A., Bellouin, N., Bopp, L., Boyd, P. W., Denier van der Gon, H. A. C.,  
603 Desboeufs, K. V., Dulac, F., Facchini, M. C., Gantt, B., Langmann, B., Mahowald, N. M., Marañón,  
604 E., O’Dowd, C., Olgun, N., Pulido-Villena, E., Rinaldi, M., Stephanou, E. G. and Wagener, T.: Ocean–  
605 atmosphere interactions of particles, in *Ocean–Atmosphere Interactions of Gases and Particles*,  
606 edited by M. T. Johnson, pp. 171–246, DOI 10.1007/978-3-642-25643-1\_4, Springer: Heidelberg.,  
607 2014.

608 Lemaitre, N., Planchon, F., Planquette, H., Dehairs, F., Fonseca-Batista, D., Roukaerts, A., Deman, F.,  
609 Tang, Y., Mariez, C. and Sarthou, G.: High variability of export fluxes along the North Atlantic  
610 GEOTRACES section GA01: Particulate organic carbon export deduced from the 234Th method,  
611 *Biogeosciences Discuss*, 1–38, doi:10.5194/bg-2018-190, 2018a.

612 Lemaitre, N., Planquette, H., Planchon, F., Sarthou, G., Jacquet, S., García-Ibáñez, M. I., Gourain, A.,  
613 Cheize, M., Monin, L., André, L., Laha, P., Terry, H. and Dehairs, F.: Particulate barium tracing of  
614 significant mesopelagic carbon remineralisation in the North Atlantic, *Biogeosciences*, 15(8),  
615 2289–2307, doi:10.5194/bg-15-2289-2018, 2018b.

616 Lherminier, P., Mercier, H., Huck, T., Gourcuff, C., Perez, F. F., Morin, P. and Sarafanov, A.: The Atlantic  
617 meridional overturning circulation and the subpolar gyre observed at the A25-Ovide section in  
618 June 2002 and 2004, *Deep Sea Res I*, 57(11), 1374–1391, doi:10.1016/j.dsr.2010.07.009, 2010.

619 Mahowald, N. M., Baker, A. R., Bergametti, G., Brooks, N., Duce, R. A., Jickells, T. D., Kubilay, N.,  
620 Prospero, J. M. and Tegen, I.: Atmospheric global dust cycle and iron inputs to the ocean, *Glob.*  
621 *Biogeochem Cy*, 19, GB4025, doi:10.1029/2004GB002402., 2005.

622 McManus, J. F., Francois, R., Gherardi, J.-M., Keigwin, L. D. and Brown-Leger, S.: Collapse and rapid  
623 resumption of Atlantic meridional circulation linked to deglacial climate changes, *Nature*, 428,  
624 834–837, 2004.

625 Measures, C. I. and Brown, E. T.: Estimating dust input to the Atlantic Ocean using surface water Al  
626 concentrations, in *The impact of African Dust across the Mediterranean*, edited by Guerzoni and  
627 Chester, p. 389, Kluwer., 1996.

628 Menzel Barraqueta, J.-L., Schlosser, C., Planquette, H., Gourain, A., Cheize, M., Boutorh, J., Shelley, R.,  
629 Contreira Pereira, L., Gledhill, M., Hopwood, M. J., Lacan, F., Lherminier, P., Sarthou, G. and  
630 Achterberg, E. P.: Aluminium in the North Atlantic Ocean and the Labrador Sea (GEOTRACES GA01  
631 section): roles of continental inputs and biogenic particle removal, *Biogeosciences*, 15(16), 5271–  
632 5286, doi:https://doi.org/10.5194/bg-15-5271-2018, 2018a.

633 Menzel Barraqueta, J.-L., Klar, J. K., Gledhill, M., Schlosser, C., Shelley, R., Planquette, H., Wenzel, B.,  
634 Sarthou, G. and Achterberg, E. P.: Atmospheric aerosol deposition fluxes over the Atlantic Ocean:  
635 A GEOTRACES case study, *Biogeosciences Discuss.*, 1–25, doi:https://doi.org/10.5194/bg-2018-  
636 209, 2018b.

637 Mercier, H., Lherminier, P., Sarafanov, A., Gaillard, F., Daniault, N., Desbruyères, D., Falina, A., Ferron,  
638 B., Gourcuff, C., Huck, T. and Thierry, V.: Variability of the Meridional Overturning Circulation at  
639 the Greenland-Portugal Ovide section from 1993 to 2010, *Prog. Oceanogr.*, 132, 250–261,  
640 <http://dx.doi.org/10.1016/j.pocean.2013.11.001>, 2015.

641 Montero-Serrano, J. C., Frank, N., Tisnérat-Laborde, N., Colin, C., Wu, C. C., Lin, K., Shen, C. C., Copard,  
642 K., Orejas, C., Gori, A., De Mol, L., Van Rooij, D., Reverdin, G. and Douville, E.: Decadal changes in  
643 the mid-depth water mass dynamic of the Northeastern Atlantic margin (Bay of Biscay), *Earth  
644 Planet Sci Lett*, 364, 134–144, 2013.

645 Moran, S. B., Shen, C.-C., Edmonds, H. N., Weinstein, S. E., Smith, J. N. and Edwards, R. L.: Dissolved  
646 and particulate  $^{231}\text{Pa}$  and  $^{230}\text{Th}$  in the Atlantic Ocean: constraints on intermediate/deep water  
647 age, boundary scavenging, and  $^{231}\text{Pa}/^{230}\text{Th}$  fractionation, *Earth Planet Sci Lett*, 203(3–4), 999  
648 1014, doi:10.1016/S0012-821X(02)00928–7, 2002.

649 Negre, C., Zahn, R., Thomas, A. L., Masque, P., Henderson, G. M., Martinez-Mendez, G., Hall, I. R. and  
650 Mas, J. L.: Reversed flow of Atlantic deep water during the Last Glacial Maximum, *Nature*, 468,  
651 84–88, 2010.

652 Pérez, F. F., Mercier, H., Vázquez-Rodríguez, M., Lherminier, P., Velo, A., Pardo, P. C., Rosón, G. and  
653 Ríos, A. F.: Atlantic Ocean  $\text{CO}_2$  uptake reduced by weakening of the meridional overturning  
654 circulation, *Nat. Biogeoscience*, doi: 10.1038/NGEO1680, 2013.

655 Pérez, F. F., Fontela, M., García-Ibáñez, M. I., Mercier, H., Velo, A., Lherminier, P., Zunino, P., Paz, M.  
656 de la, Alonso-Pérez, F., Guallart, E. F. and Padin, X. A.: Meridional overturning circulation conveys  
657 fast acidification to the deep Atlantic Ocean, *Nature*, 554(7693), 515–518,  
658 doi:10.1038/nature25493, 2018.

659 Pollard, R., Sanders, R., Lucasa, M. and Statham, P.: The Crozet Natural Iron Bloom and Export  
660 Experiment (CROZEX), *Deep Sea Res II*, 54(18–20), 1905–1914, 2007.

661 Reverdin, G., Cayan, D., Dooley, H. D., Ellett, D. J., Levitus, S., Du Penhoat, Y. and Dessier, A.: Surface  
662 salinity of the North Atlantic: Can we reconstruct its fluctuations over the last one hundred years?,  
663 *Progr Ocean.*, 33, 303–346, 1994.

664 Roca-Martí, M., Puigcorbó, V., Loeff, M. M. R. van der, Katlein, C., Fernández-Méndez, M., Peeken, I.  
665 and Masqué, P.: Carbon export fluxes and export efficiency in the central Arctic during the record  
666 sea-ice minimum in 2012: a joint  $^{234}\text{Th}/^{238}\text{U}$  and  $^{210}\text{Po}/^{210}\text{Pb}$  study, *J. Geophys. Res. Oceans*,  
667 121(7), 5030–5049, doi:10.1002/2016JC011816, 2016.

668 Sabine, C. L., Feely, R. A., Gruber, N., Key, R. M., Lee, K., Bullister, J. L., Wanninkhof, R., Wong, C. S.,  
669 Wallace, D. W. R., Tilbrook, B., Millero, F. J., Peng, T.-H., Kozyr, A., Ono, T. and Rios, A. F.: The  
670 oceanic sink for anthropogenic  $\text{CO}_2$ , *Science*, 682(305), 367– 371, 2004.

671 Savidge, G., Boyd, P., Pomroy, A., Harbour, D. and Joint, I.: Phytoplankton production and biomass  
672 estimates in the Northeast Atlantic Ocean, May-June 1990, *Deep Sea Res I*, 42(5), 599–617, 1995.

673 Schlitzer, R.: Ocean Data View, online: <https://odv.awi.de>, [24 Nov 2017], 2017.

674 Seager, R., Battisti, D. S., Yin, J., Gordon, N., Naik, N., Clement, A. C. and Cane, M. A.: Is the Gulf Stream  
675 responsible for Europe’s mild winters?, *Q J R Meteorol Soc*, 128(586), 2563–2586, 2002.

676 Shelley, R. U., Roca-Martí, M., Castrillejo, M., Sanial, V., Masqué, P., Landing, W. M., van Beek, P.,  
677 Planquette, H. and Sarthou, G.: Quantification of trace element atmospheric deposition fluxes to  
678 the Atlantic Ocean (>40°N; GEOVIDE, GEOTRACES GA01) during spring 2014, *Deep Sea Res. Part  
679 Oceanogr. Res. Pap.*, 119, 34–49, doi:10.1016/j.dsr.2016.11.010, 2017.

680 Shelley, R. U., Landing, W. M., Ussher, S. J., Planquette, H. and Sarthou, G.: Regional trends in the  
681 fractional solubility of Fe and other metals from North Atlantic aerosols (GEOTRACES cruises GA01  
682 and GA03) following a two-stage leach, *Biogeosciences*, 15(8), 2271–2288, doi:10.5194/bg-15-  
683 2271-2018, 2018.

684 Sutton, J. N., Souza, G. F. de, García-Ibáñez, M. I. and Rocha, C. L. D. L.: The silicon stable isotope  
685 distribution along the GEOVIDE section (GEOTRACES GA-01) of the North Atlantic Ocean,  
686 *Biogeosciences*, 15(18), 5663–5676, doi:<https://doi.org/10.5194/bg-15-5663-2018>, 2018.

687 Tang, Y., Castrillejo, M., Roca-Martí, M., Masqué, P., Lemaitre, N. and Stewart, G.: Distributions of total  
688 and size-fractionated particulate  $^{210}\text{Po}$  and  $^{210}\text{Pb}$  activities along the North Atlantic GEOTRACES

689 GA01 transect: GEOVIDE cruise, *Biogeosciences*, 15(17), 5437–5453,  
690 doi:<https://doi.org/10.5194/bg-15-5437-2018>, 2018.

691 Tonnard, M., Planquette, H., Bowie, A. R., van der Merwe, P., Gallinari, M., Desprez de Gésincourt, F.,  
692 Germain, Y., Gourain, A., Benetti, M., Reverdin, G., Tréguer, P., Boutorh, J., Cheize, M., Menzel  
693 Barraqueta, J.-L., Pereira-Contreira, L., Shelley, R., Lherminier, P. and Sarthou, G.: Dissolved iron  
694 in the North Atlantic Ocean and Labrador Sea along the GEOVIDE section (GEOTRACES section  
695 GA01), *Biogeosciences Discuss*, 1–53, doi:10.5194/bg-2018-147, 2018.

696 Wischmeyer, A. G., Del Amo, Y., Brzezinski, M. and Wolf-Gladrow, D. A.: Theoretical constraints on the  
697 uptake of silicic acid species by marine diatoms, *Mar Chem*, 82(1–2), 13–29, 2003.

698 Xu, X., Hulburt, H. E., Schmitz Jr., W. J., Zantopp, R., Fischer, J. and Hogan, J.: On the currents and  
699 transports connected with the Atlantic Meridional Overturning Circulation in the subpolar North  
700 Atlantic, *J Geophys Res*, in press, doi: 10.1002/jgrc.20065, 2013.

701 Zunino, P., Lherminier, P., Mercier, H., Padín, X.A., Ríos, A.F. and Pérez, F.F.: Dissolved inorganic carbon  
702 budgets in the eastern subpolar North Atlantic in the 2000s from in situ data, *Geophys. Res. Lett.*,  
703 42(22), 9853–9861, doi:10.1002/2015GL066243, 2015.

704 Zunino, P., Lherminier, P., Mercier, H., Daniault, N., García-Ibáñez, M. I. and Pérez, F. F.: The GEOVIDE  
705 cruise in May–June 2014 reveals an intense Meridional Overturning Circulation over a cold and  
706 fresh subpolar North Atlantic, *Biogeosciences*, 14(23), 5323–5342, doi:10.5194/bg-14-5323-2017,  
707 2017.

708 Zurbrick, C. M., Boyle, E. A., Kayser, R. J., Reuer, M. K., Wu, J., Planquette, H., Shelley, R., Boutorh, J.,  
709 Cheize, M., Contreira, L., Menzel Barraqueta, J.-L., Lacan, F. and Sarthou, G.: Dissolved Pb and Pb  
710 isotopes in the North Atlantic from the GEOVIDE transect (GEOTRACES GA-01) and their decadal  
711 evolution, *Biogeosciences*, 15(16), 4995–5014, doi:<https://doi.org/10.5194/bg-15-4995-2018>,  
712 2018.

713

714 **Figure captions**

715 **Figure 1:** Schematic diagram of the mean large-scale circulation adapted from Danialt et al.  
716 (Danialt et al., 2016) and Zunino et al. (Zunino et al., 2017). Bathymetry is plotted in color  
717 with color changes at 100 and 1000m and every 1000m below 1000 m. Black dots represent  
718 the Short station, yellow stars the Large ones, orange stars the XLarge ones, and red stars the  
719 Super ones. The main water masses are indicated: Denmark Strait Overflow Water (DSOW),  
720 Iceland–Scotland Overflow Water (ISOW), Labrador Sea Water (LSW), Mediterranean Water  
721 (MW), and lower Northeast Atlantic Deep Water (LNEADW).

722 **Figure 2:** Section plots for (a) salinity, (b) potential temperature ( $^{\circ}\text{C}$ ), (c) dissolved oxygen  
723 ( $\mu\text{mol kg}^{-1}$ ), (d) nitrate + nitrite ( $\mu\text{mol L}^{-1}$ ), and (e) silicic acid ( $\mu\text{mol L}^{-1}$ ) during the GEOVIDE  
724 cruise. Water masses are indicated in black, MW: Mediterranean Water; ENACW: North  
725 Atlantic Central Water; NEADW: North East Atlantic Deep Water; LSW: Labrador Sea Water;  
726 ISOW: Iceland-Scotland Overflow Water; SAIW: Sub-Arctic Intermediate Water; IcSPMW:  
727 Iceland Sub-Polar Mode Water; IrSPMW: Irminger Sub-Polar Mode Water. Station locations  
728 are indicated by the numbers on top of the panel. These plots were generated by Ocean Data  
729 View (Schlitzer, 2017).

730 **Figure 3:** Section plots for (a) biogenic silica (BSi,  $\mu\text{mol L}^{-1}$ ), (b) particulate organic carbon (POC,  
731  $\mu\text{mol L}^{-1}$ ), and (c) particulate organic nitrogen (PON,  $\mu\text{mol L}^{-1}$ ), during the GEOVIDE cruise.  
732 Station locations are indicated by the numbers on top of the panel. These plots were  
733 generated by Ocean Data View (Schlitzer, 2017).

734

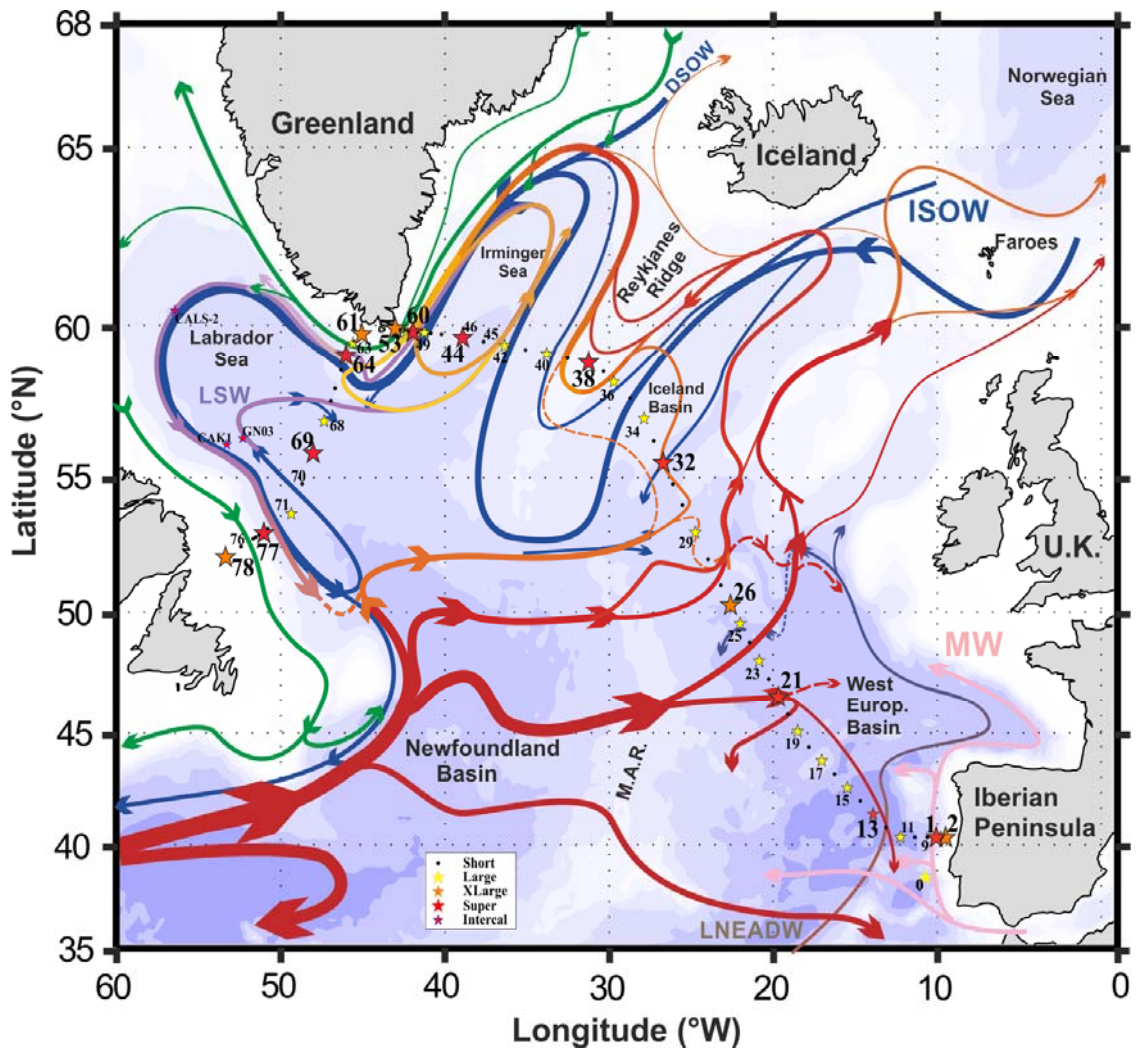
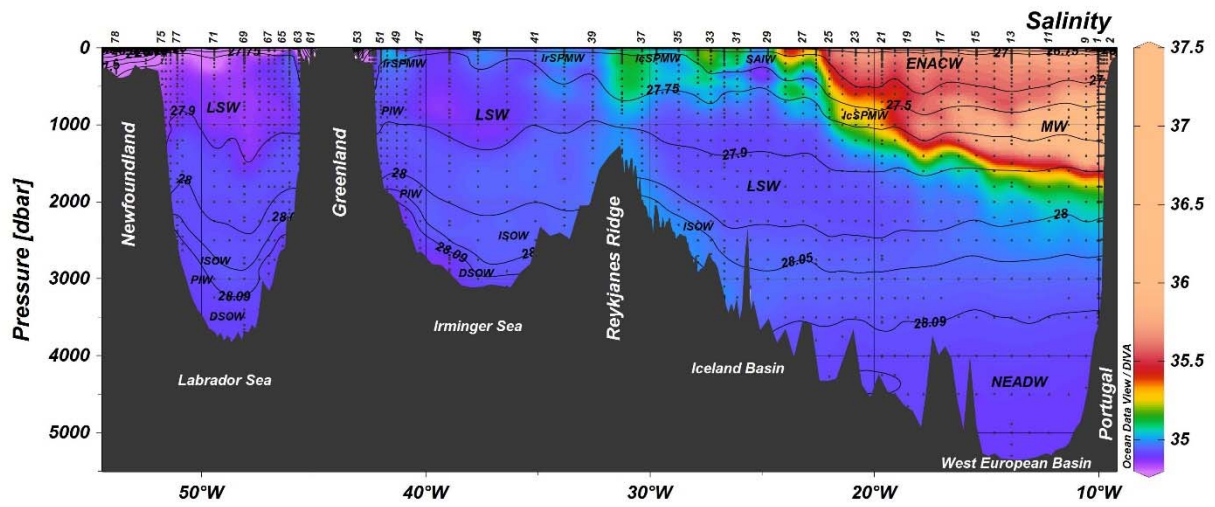
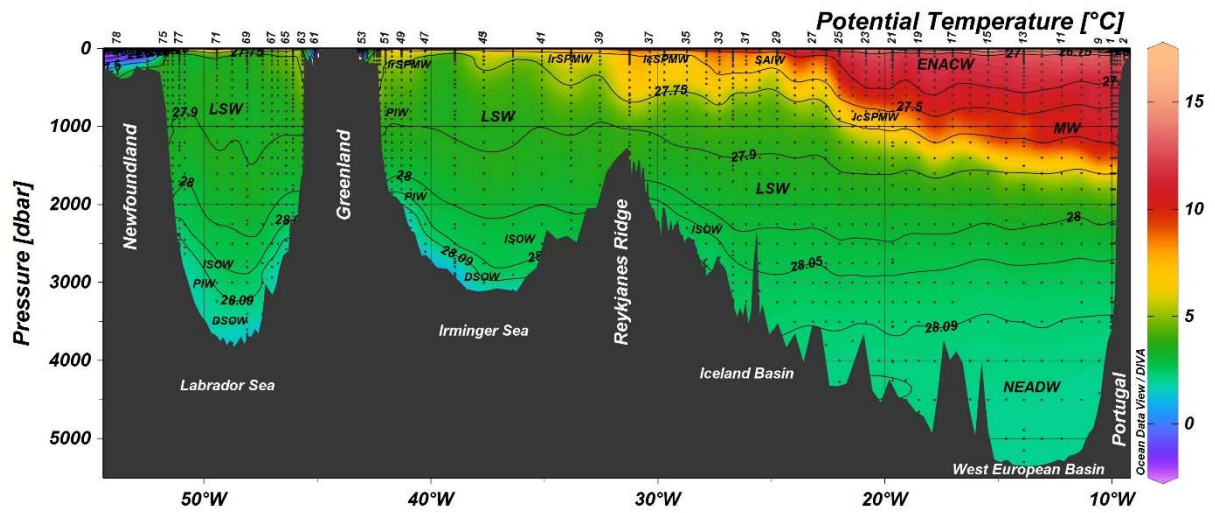


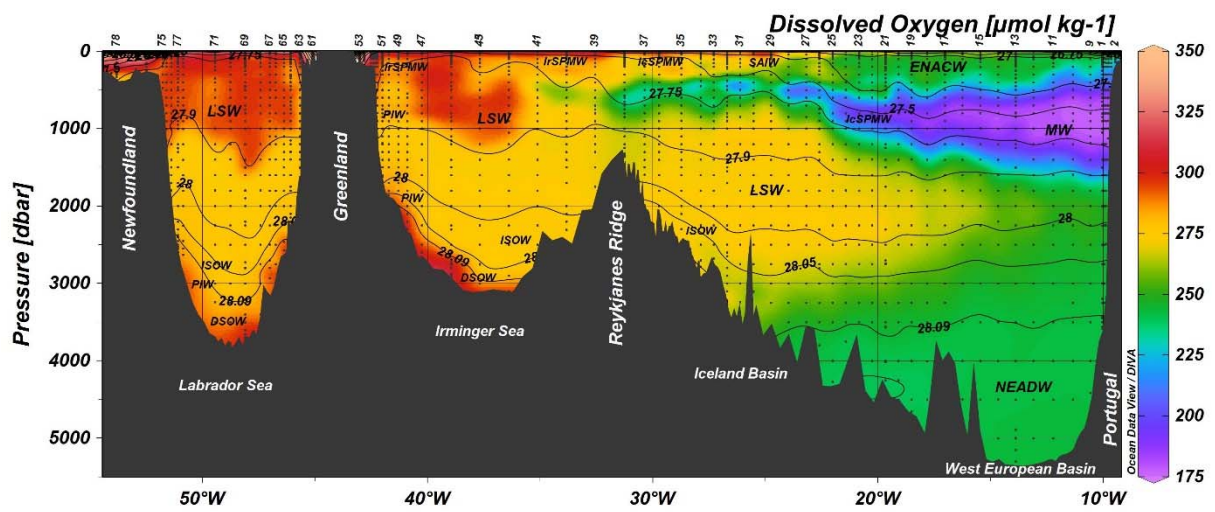
Figure 1



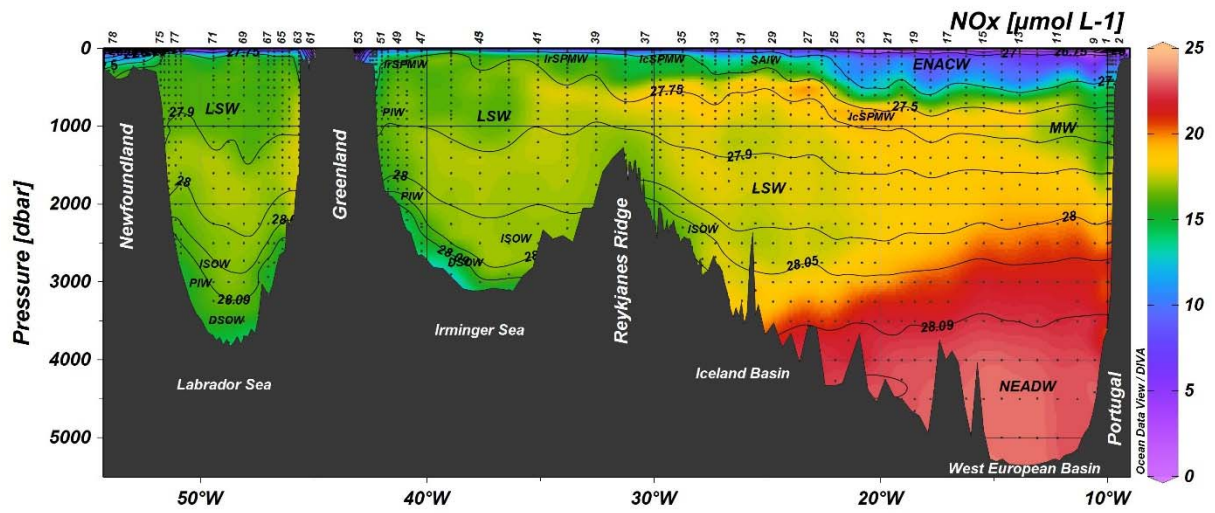
(a)



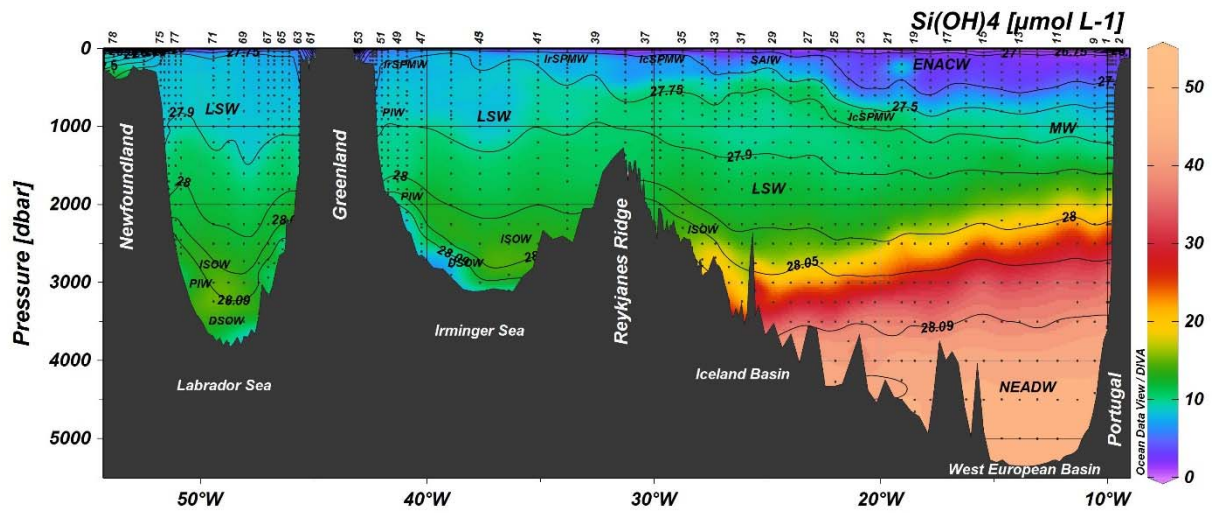
(b)



(c)

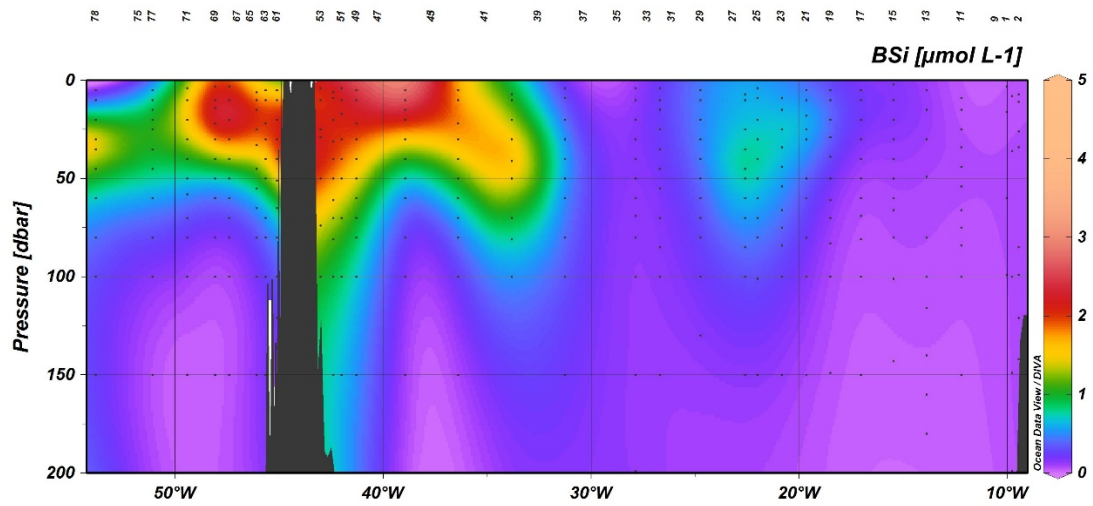


(d)

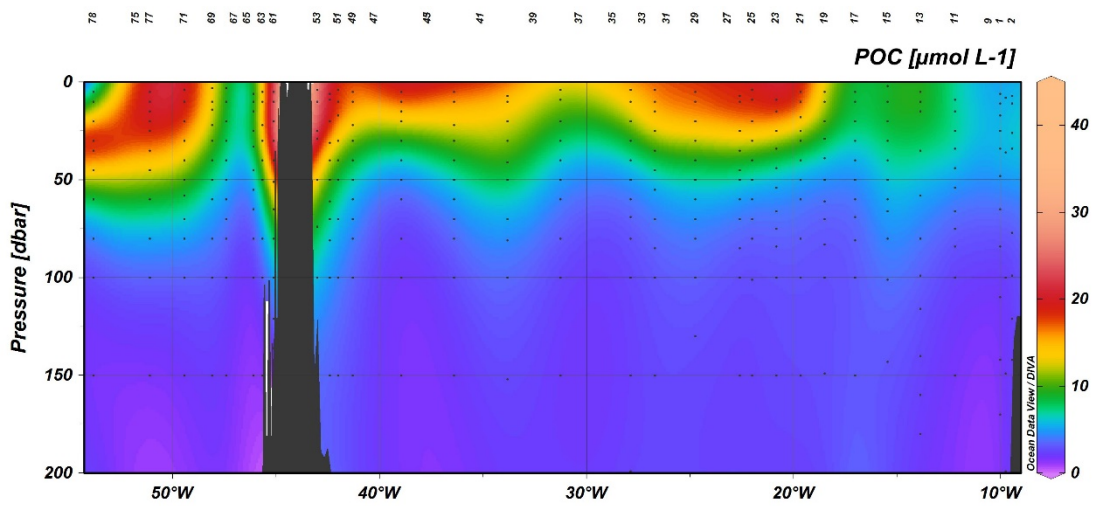


(e)

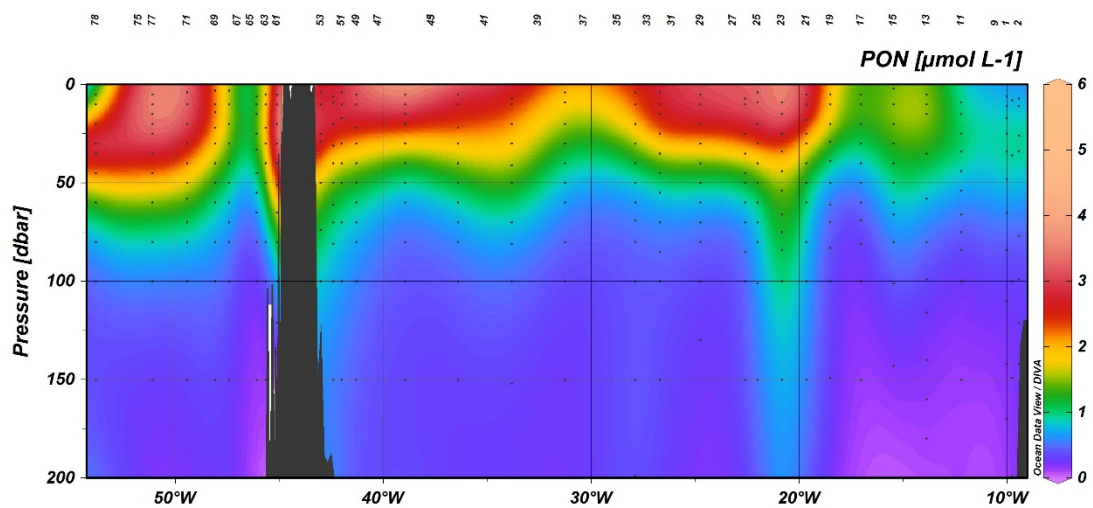
Figure 2



(a)



(b)



(c)

Figure 3